The AAPS Journal, Vol. 12, No. 3, September 2010 (© 2010)
DOI: 10.1208/s12248-010-9184-2

Research Article

Online Monitoring of PLGA Microparticles Formation Using Lasentec Focused Beam Reflectance (FBRM) and Particle Video Microscope (PVM)

Ahmed S. Zidan,[1,2] Ziyaur Rahman,[1] and Mansoor A. Khan[1,3]

Received 26 August 2009; accepted 9 March 2010; published online 30 March 2010

Abstract. Knowledge of the effects of different product and process variability on microparticle characterization is essential for the successful development, optimization, and scale-up of an encapsulation process. In the current research, the qualitative application of the Lasentec focused beam reflectance (FBRM) system for online monitoring of microparticle size distribution was demonstrated. lasentec particle vision and measurement (PVM) images were also employed to follow up the steps of microparticle formation and ripening. The drug entrapment efficiency and drug release characteristics were found to be dependent on the polymer, drug, and surfactant concentrations. DSC, FTIR, and XRD data revealed that the drug was compatible with the matrix forming polymer in the solid state. As indicated from the chord count data, FBRM was sensitive to the amount of the solid materials and the number of microparticles formed. Linear relationships with good correlations were obtained between polymer, drug, and surfactant levels and the disappearance rate of 5 to 36.8, 18.4 to 135.9, and 63 to 398 μm chord length fractions. Upon organic solvent evaporation, PVM imaging detected various stages of microemulsion droplets, sheath formation, and solidification with subsequent microparticle hardening. This study illustrated the utility of FBRM and PVM in monitoring the progress of particle formation during drug encapsulation.

KEY WORDS: biodegradable polymers; FBRM and PVM; Lasentec; microparticles; particle sizing.

INTRODUCTION

Different techniques for microencapsulation have been investigated to date; however, the selection of the appropriate encapsulation method depends on the physicochemical properties of the matrix forming material and the drug, the intended use, and the targeted length of the treatment (1). Single emulsion (*o*/*w*) solvent evaporation process is considered one of the commonly used techniques. The rate of organic solvent evaporation strongly affects the properties of the final microparticles which also depend on the miscibility of the polymer in the dispersion medium, the temperature, and its vapor pressure (2). The main factors that affect the encapsulation procedure and the final microparticles are: (a) the matrix material level, composition, and inherent viscosity; (b) the physicochemical properties of the drug being entrapped; (c) the matrix/drug weight ratio; (d) the nature of the solvent employed; (e) the level and properties of the stabilizer used; and (f) the shearing stress and the temperature of the emulsification (3,4). The published literature concerned with the online monitoring of the microparticles during its formation by the above-mentioned technique is scarce. As evolved from the process analytical technology initiative, a wide variety of process analyzer techniques is available (5). Near infrared spectroscopy and imaging, Raman spectroscopy, fiber optics, biosensors, and others are among these tools. Zidan *et al.* (6) has monitored the entrapment of a model anticancer drug, namely Anastarozole, in the final product by NIR spectroscopy and imaging. However, no information was found in the literature concerning the online monitoring of the change of particle characteristics during the solvent evaporation process.

Mettler Toledo AutoChem introduced the focused beam reflectance measurements (FBRM) that was developed by Lasentec© to measure the chord length distributions which can be correlated to the actual particle size distributions in the range of 0.25–1,000 μm. This approach allowed for online information in real time about different particles in the sample under investigation. In addition, it does not necessitate withdrawing samples or separation that can affect the actual particle size distribution due to breakdown or aggregation. For the work presented in this study, FBRM probe was used as a qualitative tool for online monitoring of the microparticle characteristics by their chord lengths during microparticles preparation. FBRM measures a chord length distribution, which is affected by the geometry, size, and number of particles under analysis (7). FBRM uses a focused beam of laser light, which scans in a circular path. As this light scans across a particle or its structure passing in front of the probe window, light is scattered in all directions. The light

[1] Division of Product Quality and Research, Center of Drug Evaluation and Research, Food and Drug Administration, White Oak, LS Building 64, Room 1070, 10903 New Hampshire Ave, Silver Spring, Maryland 20993-002, USA.
[2] Faculty of Pharmacy, Zagazig University, Zagazig, Egypt.
[3] To whom correspondence should be addressed. (e-mail: Mansoor.Khan@fda.hhs.gov)

scattered back towards the probe is used to measure a chord length off the given particle. Typically, many thousands of chords are measured per second, providing a robust measurement that is sensitive to the change in the size or number of particles under investigation (8). Unlike optical turbidity or laser diffraction, for example, FBRM does not depend on the presence of a threshold particle concentration, as soon as one particle is in the detectable size range, it will be detected. A more detailed description of the operation of the FBRM probe is available (9,10).

A particle vision and measurement (PVM) probe was also integrated into these experiments to visually monitor the steps of microparticles ripening during its preparation. PVM is a probe-based high resolution *in situ* video microscope providing images of particles and their structures as they exist in a process (8). PVM uses multiple laser lights up to six sources that can operate independently to enlighten a fixed region within the encapsulation medium. The scattered beams reflected back toward the probe are used in conjunction with a charge-coupled device element to produce an image. These images help validate particle shape and give an indication of particle dimension and structure during shearing and hardening of the microparticles (11). The current study aimed at employing both Lasentec FBRM and PVM for online monitoring of the chord length distributions of microparticle manufacturing by *o*/*w* single emulsion method using cyclosporine A (CyA) as a model drug and a medium viscosity poly(lactide-co-glycolide) (PLGA) as a matrix forming biodegradable polymer.

MATERIALS AND METHODS

Materials

Poly(lactic-co-glycolic acid) (glycolic to lactic = 50:50, MW ≈ 31,000 Da) was provided from Lactel International Absorbable Polymers (Pelham, AL, USA). Sodium lauryl sulfate (SLS) and methylene chloride were purchased from Sigma Chemical Co. (St. Louis, MO, USA). Cyclosporine A was purchased from Poli Industria Chemica S.P.A. (Rozzano, Milano, Italy).

Microparticles Preparation

CyA-loaded PLGA microparticles were formulated as described by Mok *et al.* (12) by an oil-in-water (*o*/*w*) emulsion/solvent evaporation technique. The different conditions and variables applied to various formulations are shown in Table I. Ten milliliters of methylene chloride were used to dissolve both the drug and the polymer-forming materials. SLS was used at different levels to stabilize the primary emulsion formed. The oily phase was added dropwise to 200 mL of the aqueous phase under a constant shearing stress of 400 rpm using Lightnin Stirrer (General Signal Co., NY, USA). Microparticle harvesting was done by centrifugation at 49,500 g for 30 min using Sovall/Thermo RC-5C centrifuge (Thermo Scientific, MA, USA) after washing twice with 5 mL of demineralized water followed by freeze drying in Freeze-Dry/Shell Freeze System (Labconco Corp., MI, USA). For comparison, a physical mixture of the drug and PLGA was prepared with a weight ratio that resembled batch 5, which resulted in the highest entrapment efficiency (EEF). The physical mixture was prepared by solid state mixing using mortar and pestle.

Online Chord Length Distribution Analysis and Visualization

FBRM and PVM probes from Mettler Toledo/Lasentec (Redmond, WA, USA) were positioned in the emulsification vessel to ensure good flow against the probe windows and hence allowing a representative sample of the particle system to be measured (Fig. 1). An impeller speed of 400 rpm was employed between the probes for all experiments, which helped to ensure adequate mixing, but also avoided excessive splashing in the vessel. Initially, FBRM detected no particles and the count data indicated no change in particle number. However, as soon as addition of the organic solvent started, particles were formed, and there was a corresponding increase in chord counts in the FBRM data. An advantage of using FBRM is that the measured count data can be split into specific population regions, allowing for the separation of the chord length ranges in which a change occurred. Measurement duration of 30 s was used for all FBRM analysis. As the FBRM measures over a 30-s period, the number of counts in the 1.8 to 501 μm size range was used in regions to monitor the shearing effect on the formed particles.

The PVM microscope offers a 1,320×1,760 μm field of view with a depth of approximately 1,000 μm. In order to evaluate a representative number of particles efficiently, an automatic image processing paradigm operated in MATLAB for the online PVM application during emulsification and subsequent hardening processes of the produced microparticles has been developed and used as described by De Anda *et al.* (13). Clear imaging of the microparticles under motion

Table I. Composition and Entrapment Parameters of CyA Loaded PLGA Microparticles

	Formulation variables			Entrapment parameters		
Batch no.	Polymer weight (mg)	Drug weight (mg)	SAA conc. (% *w*/*w*)	Targeted drug loading (%)	Actual drug loading (%)[a]	Entrapment efficiency (%)[a]
1	100	50	0.25	33.3	23 ± 2.7	69 ± 2.2
2	200	50	0.25	20	14 ± 0.2	72 ± 0.7
3	400	50	0.25	11.1	9 ± 1.0	82.9 ± 3.3
4	200	100	0.25	33.3	26.9 ± 1.4	80.6 ± 2.7
5	200	200	0.25	50	44.3 ± 1.0	88.5 ± 5.6
6	200	100	0.5	33.3	25 ± 2.1	75.1 ± 5.0
7	200	100	0.75	33.3	23.6 ± 0.5	70.9 ± 0.4

[a] Values ± standard deviation

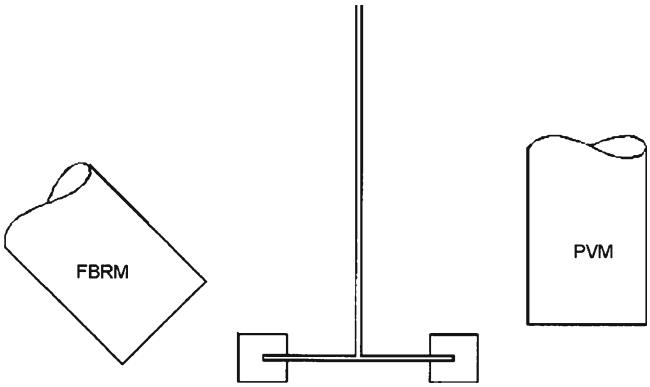

Fig. 1. Schematic drawing of probe positioning relative to the impeller

was achieved using the six independent laser sources. Uncompressed video was captured over each 5-min period during the process using the particle vision microscope, Lasentec PVM Technology System software V8.2.0 (Mettler Toledo/Lasentec, Redmond, WA, USA).

Microparticle Characterization

The surface characteristics and geometry of microparticles were scanned and analyzed by scanning electron microscopy (SEM, Nova 600 Nanolab, FEI Co, Hillsboro, OR, USA). The EEF of CyA was assessed by measuring the total amount of CyA present in freeze-dried microparticle powder and comparing this value with the theoretical core loading. For this purpose, a constant weight of the freeze-dried microparticles was dissolved in a constant volume of methylene chloride by vortexing (6). After suitable dilutions, the amount entrapped of CyA was determined using Agilent HPLC system (Hewlett Packard 1050, Agilent technologies, CA, USA) equipped with a UV detector set at 203 nm. CyA separation was done at 70°C using a reversed phase Zorbax SB-C8 column (4.6 × 250 mm, 3.5 μm packing) and a Zorbax SB-C8 reliance guard column (C8, 4.6 × 12.5 mm, 5 μm packing; Agilent technologies, CA, USA). Isocratic flow of the mobile phase composing of acetonitrile:methanol:water:phosphoric acid (8:4:3:0.05) was employed at a flow rate of 1.25 mL/min.

The microparticles were also evaluated for drug release characteristics by the horizontal shaker method. An amount of the microparticles equivalent to 5 mg of drug were suspended in 200 mL of phosphate buffer (0.20 M) pH 7.4 containing 0.1% *w/v* SLS and 0.02% *w/v* sodium azide. SLS was used to maintain sink condition and sodium azide was used to prevent the microbial growth in the release medium. Various samples were placed on a biological shaker at 37± 0.5°C and 120 rpm. Aliquots of 1 mL were withdrawn at specified time intervals (2, 4, and 8 h; 1, 2, 3, 4, 5, and 7 days) and centrifuged at 14,000 rpm for 15 min and the supernatants were analyzed for percentage of drug released by HPLC. The experiment was performed in triplicate.

Incompatibility Studies

FTIR analysis was carried out using Nicolet Impact 410 (Thermo Electron Co, Newington, NH, USA) equipped with an attenuated total reflectance accessory. The freeze-dried microparticles were scanned for absorbance over the range of 4,000 to 500 cm^{-1} wave numbers. DSC thermograms were collected using TA Thermogravimetrical Analyzer (SDT 2960 simultaneous DSC-TGA, TA Instruments Co, New Castle, DE, USA) at a heating rate of 10°C/min. XRD experiments were performed on X-ray diffractometer (MD-10 mini diffractometer, MTI Corporation, Richmond, CA, USA) using Cu K 2α rays (λ = 1.54056 Å) with a voltage of 25 KV and a current of 30 mA, in flat plate θ/2θ geometry, over the 2θ ranges 25–70°, with a step width 0.05° and a scan time of 2.0 s per step. Diffraction patterns for CyA, PLGA, physical mixture of drug, and PLGA and drug loaded nanoparticles were obtained.

RESULTS AND DISCUSSION

Microparticles Characterization

SEM photomicrograph of PLGA microparticles (batch 1) is shown in Fig. 2. For this analysis, the particles were dehydrated prior to observation by vacuum drying overnight at room temperature. It is clearly seen that PLGA microparticles were spherical with smooth surfaces and very slight aggregation, indicating that the selected stabilizer at the applied concentration did not change the particle surface characteristics. The entrapment parameters expressed as the actual and theoretical drug loadings and EEF are represented in Table I. Actual drug loadings were >69% of the theoretical drug loadings in all cases. This degree of loading, also reported in the literature (14), can be explained by the poor diffusability of CyA out of the primary emulsion due to its poor aqueous solubility (15), the interface being in this case the air introduced as a result of the turbulence produced by the impeller action. Increasing both the nominal CyA content and the polymer loading at constant drug content increased EEF whereas a negative effect was found for increasing the stabilizer concentration in the emulsification medium at constant levels of the drug and the polymer. For example, 72.0% and 88.5% were the EEFs obtained for microparticles prepared with theoretical drug loadings of 50 and 200 mg at 200 mg PLGA loading and

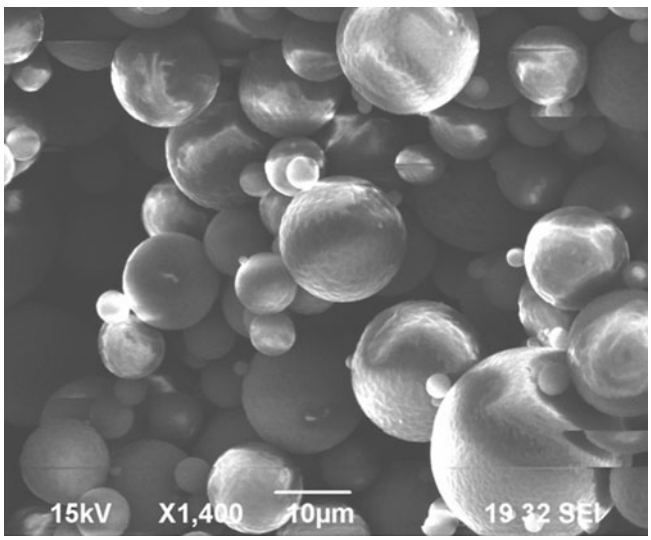

Fig. 2. The SEM morphology of CyA loaded PLGA microparticles (batch 1)

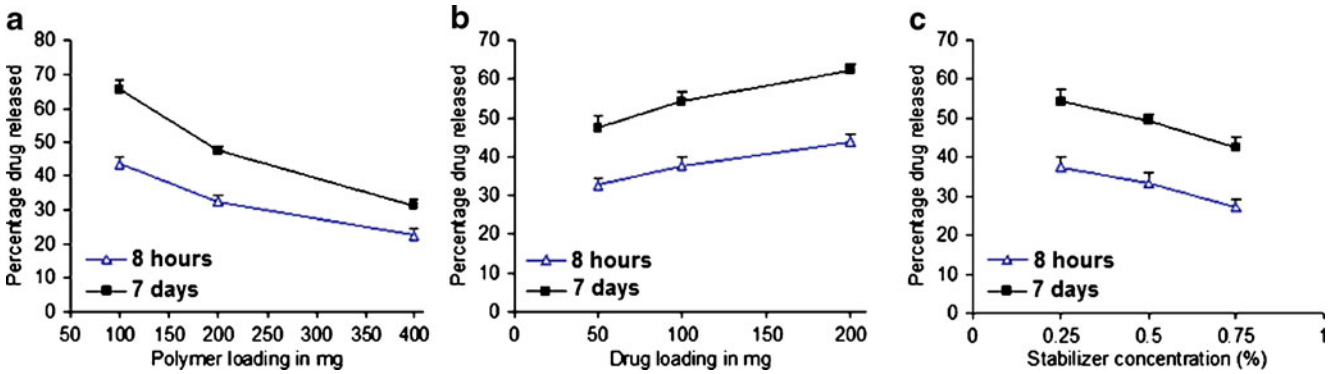

Fig. 3. Effect of changing **a** polymer loading, **b** drug loading, or **c** stabilizer concentration on the percentage of drug released from tablets after either 1 or 7 days, respectively

0.25% stabilizer concentration, respectively. The percentage of the drug loss during the preparation steps could explain the decreased EEF at lower level of the drug compared to its higher level during preparation (16). Increasing PLGA level from 100 to 400 mg resulted in an enhancement in the EEF from 69.0% to 82.9% at constant theoretical drug loading of 50 mg and constant stabilizer concentration of 0.25%, respectively. The highest entrapment by increasing PLGA mass was a result of increasing the viscosity of the internal phase that minimized the drug diffusion to the aqueous phase (17). On the contrary, a reduction in the EEF by increasing the stabilizer concentration in the emulsification medium could be attributed to the emulsification of the drug in the formed SLS micelles in the external aqueous media (6,18).

The *in vitro* release of CyA from microparticles in phosphate buffer of pH 7.4 showed a typical biphasic release pattern of a sustained/controlled release formulation, an initial burst release followed by prolonged release. The initial fast release was due to the presence of surface drug molecules which could be ascribed to solvent evaporation that caused drug precipitation at the surface of the formed microparticles (19). For determining the effects of polymer loading, drug loading, and stabilizer concentration, the percentage of drug released at two time points from the release profiles were selected, (a) after 8 h to represent the burst effect and (b) after 7 days to indicate the extent of drug dissolution within 1 week (Fig. 3). An enhancement in the drug release rate was observed by increasing the drug loading during microparticles fabrication. At higher level of the drug in the microparticles, a shorter path length was expected as a result of the surface drug molecules leaching out into the release medium. Empty pores were formed that facilitated the leaching out of the drug molecules located in the

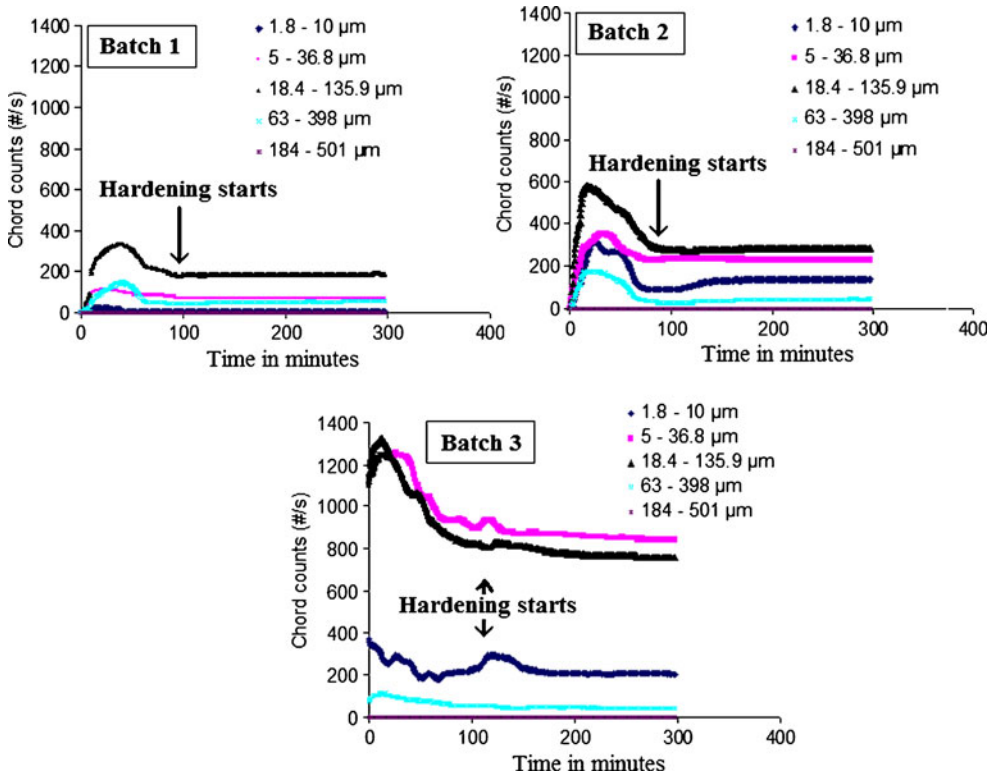

Fig. 4. Effect of polymer loading on FBRM data during microparticles formation

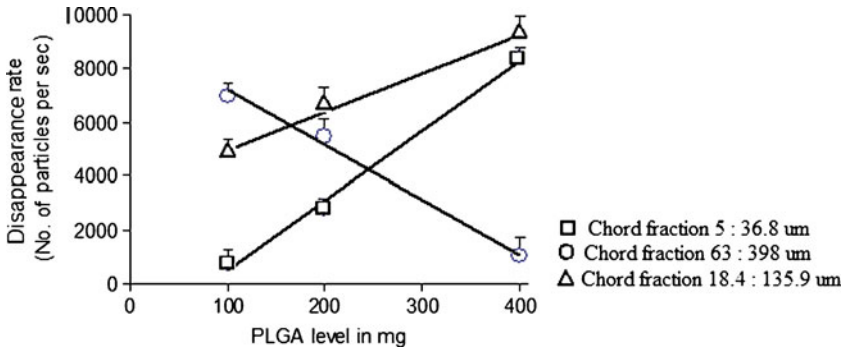

Fig. 5. Effect of polymer loading on the disappearance rate of 5 to 36.8 μm, 18.4 to 135.9 μm, and 63 to 398 μm chord length fractions during microparticles formation

core of the microparticle (20). Increasing the amount employed of PLGA during the fabrication process led to a decrease in both the burst effect and the extent of drug dissolution after 7 days. This result could be attributed to the increased viscosity of the internal medium by increasing the polymer concentration. Crow *et al.* (21) explained this observation by the effect of polymer mass and viscosity to decrease the permeability of the polymer with subsequent decrease in the drug release rate. An inverse relationship was found between the percentage of the drug released and stabilizer level in the external phase.

Online Chord Length and Visualization

In this study, the Lasentec© D600L FBRM was used for a qualitative online monitoring of the shift in the chord length distributions at various stages of microparticles ripening at a shearing stress of 400 rpm. This technique has the advantage of measuring the number of chord lengths over each range independently of other ranges (22). For spherical matrices, theoretical and empirical algorithms are available in the literature for converting chord count data to diameter data, and the empirical algorithm was found to be more precise (23). Since the main focus of this study was to monitor the microparticle formation, the conversion of the chord count data into particle size was not carried out. The measured count data can be split into specific population regions, allowing for the separation of the chord length range in which a change occurred. Figure 4 shows that the chord counts increased significantly by increasing the polymer loading from 100 to 400 mg at constant drug loading of 50 mg. This result can be attributed to the increase in the total solid content as the amount of the polymer increased and hence more particles were formed. The chord lengths were represented as nonweighted distributions in five size ranges as follows: (1) 1.8 to 10 μm fraction, (2) 5 to 36.8 μm fraction, (3) 18.4 to 135.9 μm fraction, (4) 63 to 398 μm fraction, and (5) 184 to 501 μm fraction. Initially as the organic solution was added, FBRM detected an increase in the rate of formation of all chord length ranges followed by a disappearance phase where the chord counts decreased for all chord length ranges. The disappearance phase was probably reflected either the breakdown of the coarse particles into fines or the agglomeration of the fine particles into larger ones. A plateau phase followed the disappearance phase indicated that no change in the chord counts with time was observed as the shearing stress continued. This plateau phase was indicative of hardening of the polymeric sheath of the microparticles which were not subjected to further shearing effects (Fig. 4). Focusing on the region around the start of the plateau phase (Fig. 4) showed that shearing of the formed primary emulsion was occurred at about 100 min after which no change in chord length distribution was observed. This finding illustrated the sensitivity of FBRM to the shearing effect and events associated with microparticle hardening.

Three ranges in chord length were selected to monitor the effect of increasing the polymer loading on the chord length distribution of batches 1, 2, and 3. The two extreme chord length ranges, 1.8 to 10 μm and 184 to 501 μm fractions, were present at a very low chord counts so that both were neglected. The chord ranges of 5 to 36.8 μm and 18.4 to

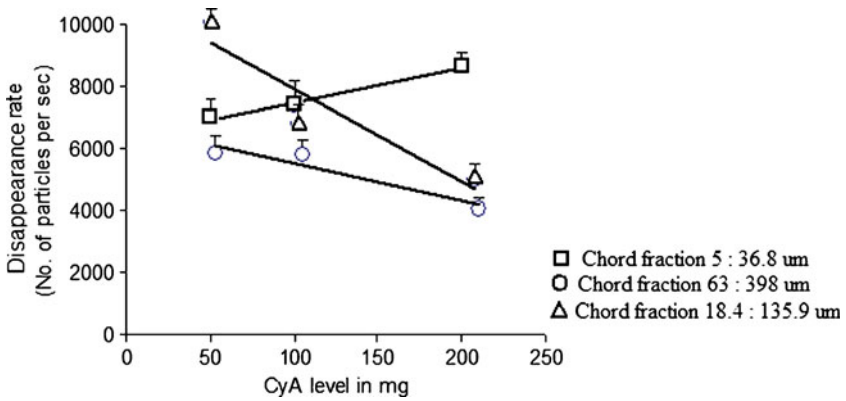

Fig. 6. Effect of drug loading on the disappearance rate of 5 to 36.8 μm, 18.4 to 135.9 μm, and 63 to 398 μm **chord length** fractions during microparticles formation

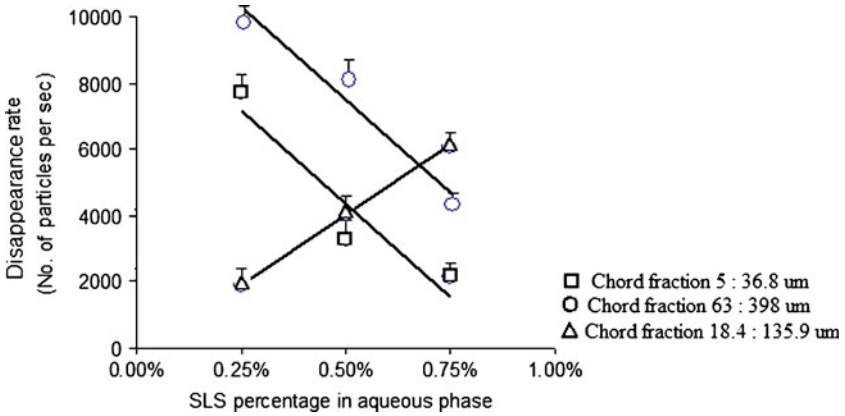

Fig. 7. Effect of stabilizer concentration in the emulsification medium on the disappearance rate of 5 to 36.8 μm, 18.4 to 135.9 μm, and 63 to 398 μm chord length fractions during microparticles formation

135.9 μm were designated to represent the fine and intermediate microparticles, respectively, while the chord length fraction covering 63 to 398 μm represented the coarse microparticles. Immediately following the formation phase, FBRM showed a rapid increase in coarse chords counts indicating the presence of large microparticles through rapid agglomeration. No specific trend was observed for the effect of polymer loading on the formation phase of the three chord length fractions. Figure 5 shows linear relationships (R^2> 0.991) between PLGA loading and the disappearance rate of these chord length factions. Disappearance rates were calculated from the slopes obtained by regressing the chord counts during the disappearance phase against time. Figures 5, 6, and 7 showed the time-dependent changes of chord counts for other batches studied. Increasing PLGA loading was accompanied by increasing the disappearance rate of both the fine and intermediate chord length fraction while decreasing that of the coarse chord length fraction. In this case, disappearance of the fine and intermediate particles could be caused by coalescence to coarse particles. Figure 8 depicts the effect of drug loading on FBRM data at constant polymer loading and stabilizer concentration (batches 2, 4, and 5). Compared to the polymer loading effect, the total number of the chord counts was almost the same and were not affected by the change in the drug loading. This result was attributed to the comparable amounts of the solid materials as some drug leached to the aqueous phase leaving out nearly the same number of particles. The same behavior was observed for the progress of microparticles formation to have three phases (formation, disappearance then plateau phase). Figure 6 shows the effect of drug loading on the disappearance rate of the three selected chord length fractions during microparticle formation showing linear relationships (R^2>0.877) within the range studied. The disappearance rate of fine chord length increased by increasing drug loading while those for both intermediate and coarse chord lengths decreased under the same condition. The increase in the coarse chord length fraction with increasing both drug and polymer loadings have been observed by others for PLGA polymers (24,25). This result can be explained by the higher viscosity of the emulsion droplets and hence reduced dispersibility of the organic phase into the aqueous medium. The viscous emulsion represented a higher resistance to the shearing stress whereby coarser particles were produced as a result of the coalescence of small particles in a more concentrated solution (26).

Varying the stabilizer concentration in the emulsification medium changed the chord length distributions at constant drug and polymer loadings (batches 4, 6, and 7). Figure 9 shows the changes in microparticle formation as a function of changing the surfactant concentration in the external aqueous phase. Compared to the polymer effect, a reduction in the total chord counts was observed as the stabilizer concentration increased. In the absence of a stabilizer in the external phase, a low yield of microparticles would be observed due to particle aggregation or the solubilization of the hydrophobic

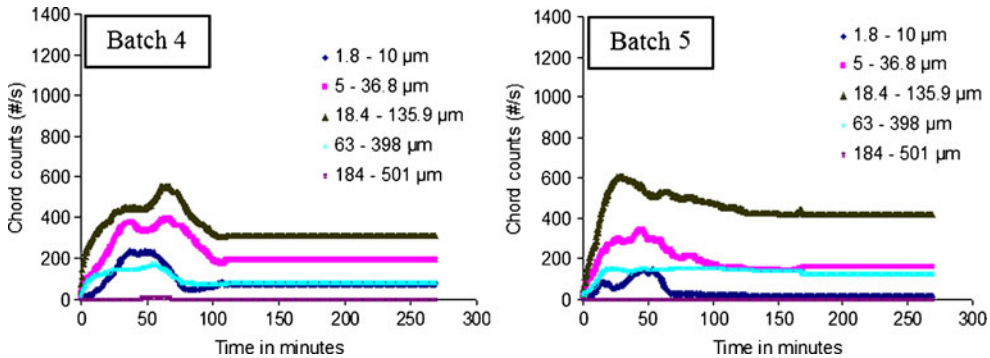

Fig. 8. Effect of drug loading on FBRM data during microparticles formation

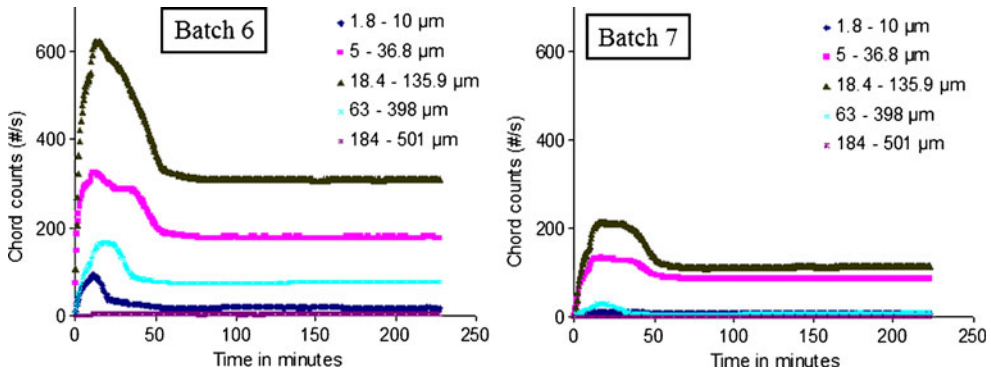

Fig. 9. Effect of stabilizer concentration on FBRM data during microparticles formation

species via micelle formation (6,27). Therefore, an optimum amount of the surfactant was required to prevent aggregation while maintaining a considerable yield. Linear relationships (R^2>0.890) were obtained between stabilizer concentration and the disappearance rate of the three ranges of chord length studied (Fig. 7). Data shown in Figs. 4, 5, 6, 7, 8, and 9 indicated FBRM can monitor the change in the chord counts and lengths sensitively within the investigated design space.

The process of ripening the microparticles during solvent evaporation was further monitored by PVM imaging (Fig. 10). The stages expressing the progress of microparticles formation were the same for all batches. Images taken each 20 min were concatenated in Fig. 10 to follow this progress. Upon completing the organic phase addition to the emulsification medium, the internal phase was compressed by the shear force into an elliptical shape then separated into

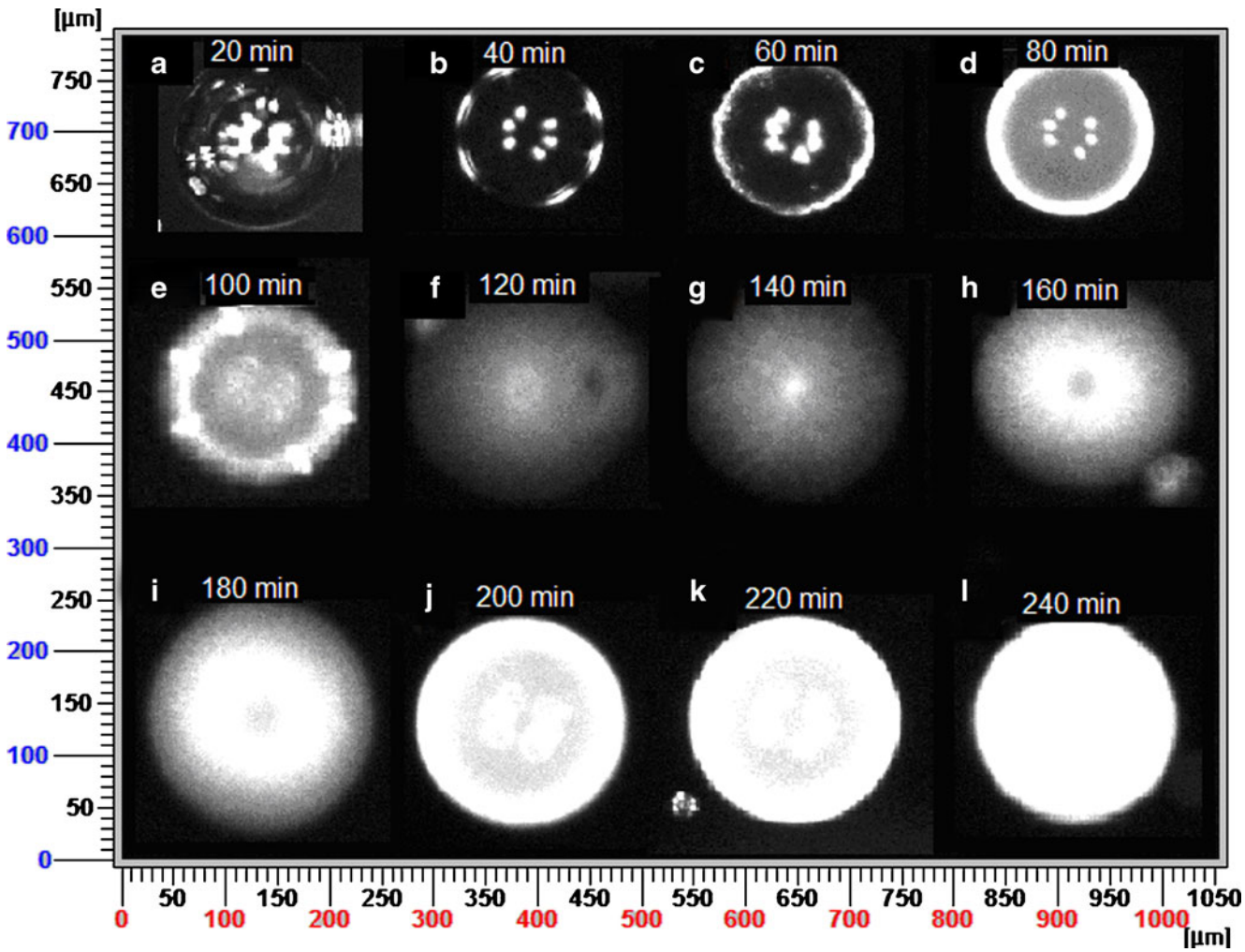

Fig. 10. PVM images taken within 4 h (20 min interval) of organic phase addition to the emulsification medium to follow up the stages of microparticle ripening of batch 1

monodisperse spherical microemulsion droplets. The droplets did not show signs of aggregation indicating that the aggregation observed in SEM images was due to the preparation method rather than insufficient stabilization by the surfactant. As the organic solvent evaporated, insoluble PLGA started to form at the droplet surface developing a sheath around the particles. At the same time, drug precipitation at the microparticle surface contributed to sheath hardening (Fig. 10, images A–D). Subsequently, an array of the insoluble polymer could be observed along the microparticle diameter as solvent evaporation continued (Fig. 10, images E–I). A hard sheath was formed around the microparticle in about 100 min after which no change in the chord length distribution as organic solvent diffused through this shell. Complete solvent evaporation and subsequent microparticle hardening was observed after 4 h where particles looked opaque with no signs of any liquid/liquid dispersion. These results indicated that PVM was able to follow the process of microparticles ripening. We demonstrated here, for the first time, that Lasentec FBRM and PVM were used successfully for the qualitative online monitoring and visualization of the effect of three formulation variables on particle size distribution.

Drug Polymer Incompatibility Studies

To further investigate any possible interaction that may exist between CyA and PLGA, FTIR, DSC, and XRD analysis were employed (Fig. 11). For this purpose, the thermograms of individual components were compared to those of the physical mixture and the microparticles. It is reported that CyA shows a characteristic melt peak at 190°C for an orthorhombic crystal form and around 110°C for a tetragonal form (28). PLGA thermogram showed an inflection point at 51.6°C indicating its glass transition temperature. This is in accordance with the observations describing the effect of cryoprotectants on the thermal behavior of PLGA-based nanoparticles (29). DSC thermogram of the raw CyA showed no peak indicating the amorphous nature of the drug. The same finding was observed in the thermograms of the physical mixture and the microparticles where no extra endo/exothermic thermal transitions indicating no interaction existed between PLGA and CyA by the formulation method employed. The results of XRD analysis fortified this observation to indicate the amorphous nature of individual components as well as both the physical mixture and freeze-dried microparticles powder (Fig. 11).

In order to investigate any possible chemical interactions, FTIR analysis was employed in the current investigation (Fig. 11). The spectra of the raw CyA as well as its physical mixture and microparticles freeze-dried powder showed characteristic peaks at 2,873 and 2,836 cm^{-1} correspond to the aliphatic C-H stretching vibration and at 1,680 cm^{-1} corresponds to its carbonyl stretch. Raw PLGA spectrum showed a characteristic stretch at 1,715 cm^{-1} indicating its carbonyl stretch. The position of the absorbance bands remained the same in the spectra of the physical mixture or freeze-dried microparticle powder indicating the chemical compatibility of the drug with the investigated matrix. Bertacche *et al.* (30) stated that the crystalline form of CyA shows characteristic peak at

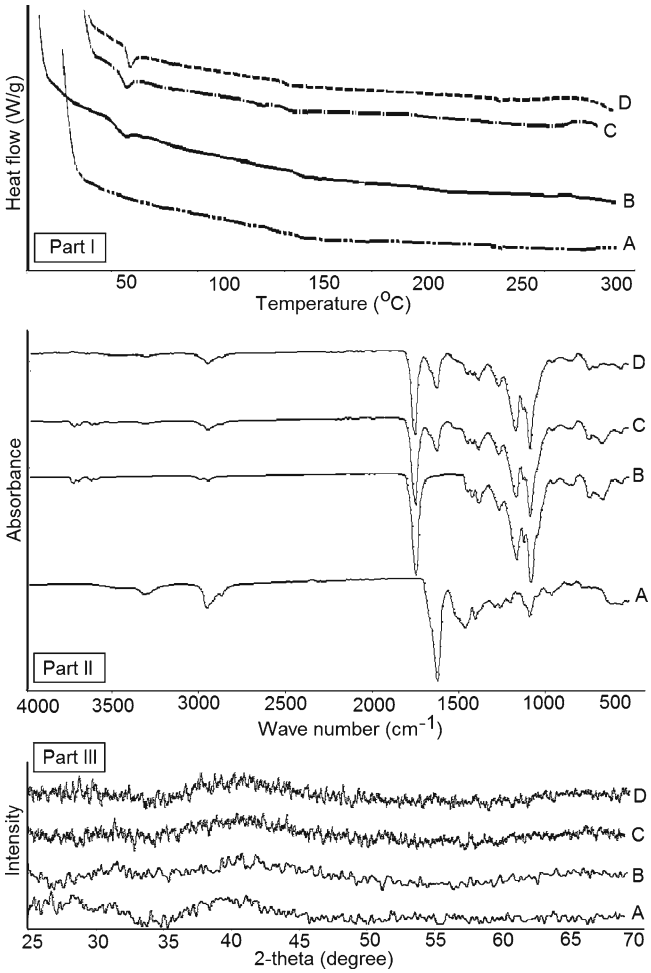

Fig. 11. DSC thermograms (*part I*), FTIR spectra (*part II*), and XRD patterns (*part III*) of *a* CyA, *b* PLGA, *c* physical mixture, and *d* batch 5 of CyA loaded microparticles

2,855 cm^{-1} and another peak at 2,928 cm^{-1} that shifted to 2,836 cm^{-1} in amorphous form. FTIR data confirmed those obtained by DSC and XRD to indicate that CyA entrapment within PLGA microparticles was a physical process with no incompatibilities. Therefore, the process under investigation is a physical process and no new chemical entities were formed.

CONCLUSION

The FBRM technology was successfully employed as a powerful and convenient process analyzer for the qualitative online monitoring of the shift in the microparticle chord length distribution during its fabrication. The incompatibility study should a homogenous matrix with no chemical interactions. Both FBRM and PVM offered the advantage of not only the sensitivity for detecting the shearing time, but also tracking the fine and coarse microparticles during formulation. PVM images helped to illustrate the shape of the microparticles, but more importantly showed the steps of microparticle ripening during solvent evaporation. This should serve as a useful parameter to help assess the effect of different process variables on the progress of these steps and subsequent scale-up.

ACKNOWLEDGMENT

The authors would like to acknowledge the Oak Ridge Institute for Science and Education (ORISE) for its support with a research postdoctoral fellowship. The views presented in this article do not necessarily reflect those of the US Food and Drug Administration.

REFERENCES

1. Jain RA. The manufacturing techniques of various drug loaded biodegradable poly(lactide-co-glycolide) (PLGA) devices. Biomaterials. 2000;21(23):2475–90.
2. Arshady R. Preparation of biodegradable microspheres and microcapsules: 2. Polylactides and related polyesters. J Control Rel. 1991;17:1–22.
3. Jalil R, Nixon JR. Biodegradable poly(lactic acid) and poly (lactide-co-glycolide) microcapsules: problems associated with preparative techniques and release properties. J Microencapsulation. 1990;7:297–325.
4. Lewis DH. Controlled release of bioactive agents from lactide/glycolide polymers. In: Chasin M, Langer R, editors. Biodegradable polymers as drug delivery systems. New York: Marcel Dekker; 1990. p. 1–41.
5. Guidance for Industry. PAT—A framework for innovative pharmaceutical development, manufacturing, and quality assurance. 2004. http://www.fda.gov/downloads/Drugs/GuidanceComplianceRegulatoryInformation/Guidances/UCM070305.pdf
6. Zidan AS *et al*. Process analytical technology: non-destructive assessment of anastrozole entrapment within PLGA microparticles by near infrared spectroscopy and chemical imaging. J Microencapsulation. 2008;3:145–53.
7. Barrett P, Glennon B. In-line FBRM monitoring of particle size in dilute agitated suspensions. Part Part Syst Charact. 1999;16:207–11.
8. Barrett P, Glennon B. Characterizing the metastable zone width and solubility curve using Lasentec FBRM and PVM. Chem Eng Res Des. 2002;80(7):799–805.
9. Sparks RG, Dobbs CL. The use of laser backscatter instrumentation for the on-line measurement of particle size distribution for emulsions. Part Part Sys Charact. 1993;10:279–89.
10. Tadayyon A, Rohani S. Determination of particle size distributionby Partec 100: modeling and experimental results. Part Part Sys Charact. 1998;15:127–35.
11. Kempkes M, Eggers J, Mazzotti M. Measurement of particle size and shape by FBRM and *in situ* microscopy. Chem Eng Sci. 2008;63(19):4656–75.
12. Mok H, Park TG. Direct plasmid DNA encapsulation within PLGA nanospheres by single oil-in-water emulsion method. Eur J Pharm Biopharm. 2008;68(1):105–11.
13. De Anda JC, Wang XZ, Roberts KJ. Multi-scale segmentation image analysis for the in-process monitoring of particle shape with batch crystallisers. Chem Eng Sci. 2005;60(4):1053–65.
14. Bittner B *et al*. Recombinant human erythropoietin (rhEPO) loaded poly(lactide-co-glycolide) microspheres: influence of the encapsulation technique and polymer purity on microsphere characteristics. Eur J Pharm Biopharm. 1998;45:295–305.
15. Lallemand F *et al*. A water-soluble prodrug of cyclosporine A for ocular application: a stability study. Eur J Pharm Sci. 2005;26(1):124–9.
16. Sandor M *et al*. Effect of protein molecular weight on release from micron-sized PLGA microspheres. J Control Release. 2001;76:297–311.
17. Wang D *et al*. Encapsulation of plasmid DNA in biodegradable poly(D, L-lactic-coglycolic acid) microspheres as a novel approach for immunogene delivery. J Control Release. 1999;57:9–18.
18. Yang Q, Owusu-Ababio G. Biodegradable progesterone microsphere delivery system for osteoporosis therapy. Drug Dev Ind Pharm. 2000;26:61–70.
19. Jalil R, Nixon JR. Microencapsulation using poly(l-lactic acid) I: microcapsule properties affected by the preparation technique. J Microencapsulation. 1989;6:473–84.
20. Chen S, Singh J. Controlled delivery of testosterone from smart polymer solution based systems: *in vitro* evaluation. Int J Pharm. 2005;295:183–90.
21. Crow BB *et al*. Evaluation of *in vitro* drug release, pH change, and molecular weight degradation of poly(L-lactic acid) and poly (D, L-lactide-co-glycolide). Tissue Eng. 2005;11:1077–84.
22. Kougoulos E, Jones AG, Wood-Kaczmar MW. Modelling particle disruption of an organic fine chemical compound using Lasentec focussed beam reflectance monitoring (FBRM) in agitated suspensions. Powder Technol. 2005;155(2):153–8.
23. Heath AR *et al*. Estimating Average Particle Size by Focused Beam Reflectance Measurement (FBRM). Part Part Syst Charact. 2002;19(2):84–95.
24. Kwon HY *et al*. Preparation of PLGA nanoparticles containing estrogen by emulsification-diffusion method. Colloids Surf A: Physicochem Eng. 2001;182:123–30.
25. Chorny M *et al*. Lipophilic drug loaded nanospheres prepared by nanoprecipitation: effect of formulating variables on size, drug recovery and release kinetics. J Control Release. 2002;83:389–400.
26. Quintanar-Guerrero D *et al*. Influence of stabilizing agents and preparative variables on the formation of poly(d, l-lactic acid) nanoparticles by an emulsification-diffusion technique. Int J Pharm. 1996;143:133–41.
27. Feng S, Huang G. Effects of emulsifiers on the controlled release of paclitaxel (Taxol®) from nanospheres of biodegradable polymers. J Control Release. 2001;71:53–69.
28. Lechuga-Ballestros D *et al*. Properties and stability of a liquid crystal form of Cyclosporine—the first reported naturally occurring peptide that exists as a thermotropic liquid crystal. J Pharm Sci. 2003;92:1821–31.
29. Holzer M *et al*. Physico-chemical characterisation of PLGA nanoparticles after freeze-drying and storage. Eur J Pharm Biopharm. 2009;72(2):428–37.
30. Bertacche V *et al*. Quantitative determination of amorphous cyclosporine in crystalline cyclosporine samples by Fourier transform infrared spectroscopy. J Pharm Sci. 2005;95:159–66.